Meeting the Needs of a Potent Carrier for Malaria Treatment: Encapsulation of Artemisone in Poly(lactide-*co*-glycolide) Micro- and Nanoparticles

Mina Heidari, Jacob Golenser, and Andreas Greiner*

Biodegradable polymer nano- and microparticles are of interest as drug carriers due to their capability to modulate drug release. Two different methods, including solvent displacement and spray drying, are used, resulting in the fabrication of Artemisone (ART)-loaded polymeric nano- and microparticles, respectively. Scanning electron microscopy, transmission electron microscopy, dynamic light scattering, and asymmetric flow field flow fractionation (AF4) are employed to evaluate the morphology and size of the particles. The encapsulation and loading efficiency of the drug as well as cumulative release are characterized using high-performance liquid chromatography (HPLC). HPLC results confirm that the spray drying method provides higher encapsulation efficiencies of about 97%, whereas, in nanoparticles prepared by solvent displacement, the highest encapsulation efficiency is 71%. Using these production methods, round-shaped particles with homogeneous size distribution are fabricated. Moreover, the preparation procedure is optimized to obtain particles with the highest encapsulation and drug loading efficiency. Using the solvent displacement method, stable dispersions in water are obtained without adding any surfactant, whereas, for spray-dried microparticles, tween 80 is needed to redisperse particles. The micro- and nanoparticles show different release properties, which are of interest for drug delivery application of hydrophobic drugs like ART.

1. Introduction

Malaria is globally known as one of the most dangerous infectious disease, caused by plasmodium parasites.[1,2] It leads to

M. Heidari, A. Greiner
University of Bayreuth Macromolecular Chemistry
and Bavarian Polymer Institute
Universitätsstraße 30, Bayreuth 95440, Germany
E-mail: greiner@uni-bayreuth.de
J. Golenser
Department of Microbiology and Molecular Genetics
The Kuvin Centre for the Study of Infectious and Tropical Diseases
The Hebrew University of Jerusalem, 919041
Jerusalem, Israel

The ORCID identification number(s) for the author(s) of this article can be found under https://doi.org/10.1002/ppsc.202100152.

the death of about 435 000 people especially in tropical and subtropical regions.[3] Among artemisinin derivatives, artemisone (ART) is considered a most potent agent for treatment of malaria, owing to its lack of neurotoxicity, anti-plasmodial, anti-inflammatory, and significant therapeutic effect against cerebral malaria. Most importantly, it is not converted to dihydroxyartemisinin, to which some parasite resistance was found.[4–6] Additionally, ART is regarded as a crystalline drug with a hydrophobic structure.[5,6] The main concern related to ART is its low bioavailability and its poor solubility in aqueous solutions.[7] To overcome these drawbacks, studies have been carried out to incorporate the drug into various types of nano- and microcarriers.[8–10] Different types of carriers such as liposomes and polymeric particles have been evaluated for the controlled delivery of drugs.[11–13] Specifically, great attention is drawn toward the polymeric nano- and microparticles as drug delivery systems due to their controlled and sustained drug delivery behavior.[14–16]

In comparison with free drugs, polymeric particles exhibit some advantages ranging from improved drug bioavailability to the ability of releasing the drug in a controlled manner and being compatible with varying administration routes. Compared with liposomes, polymeric particles have the advantage of increased storage capacity, lower cytotoxicity,[15,18] improved in vivo stability[19] against enzymatic degradation[11] and increased drug solubility in aqueous medium,[20] reducing drug side effects.[21] These lead to extended drug circulation time, lower dosing frequency and consequently and most important increased patient compliance.[22,23]

Poly(lactide-*co*-glycolide) (PLGA), an aliphatic polyester which is known as a biocompatible and biodegradable polymer has been widely used for nanoparticle fabrication and drug delivery systems.[24–26] It hydrolyzes within the body, to produce glycolic acid, which is a nontoxic biodegradable monomer.[27] Characteristics such as particle size, zeta potential, and drug loading could be tuned accurately by changing the type and quantity of polymer, amount of drug, solvent, and surfactant.[17] The resulting size of the particle is of great importance, as it plays a significant role in the stability of the particle dispersion, drug release, and cellular uptake. For an efficient drug delivery,

it is important to achieve high loading and encapsulation efficiency, as it may extend the duration and dosage of the drug as well as hampering the loss of valuable drug.[28,29]

Among versatile methods of preparing polymeric nano- and microparticles, solvent-displacement and spray drying has gained lots of interest. In the solvent-displacement method, which is principally used for lipophilic drugs, the drug and polymer are dissolved in an organic water-miscible solvent. The organic phase is then slowly added to an aqueous medium which may or may not contain surfactant, under mild stirring. This results in the spontaneous formation of emulsion droplets as a matter of the diffusion of acetone into the aqueous phase.[30] With solvent diffusing out of droplets, the size would be considerably reduced to the nanoscale. Within the following step of solvent evaporation, the droplets would be solidified, thus forming polymeric nanoparticles.[11,31–33] Different parameters could govern morphology size, size distribution, and encapsulation efficiency.[18,32] As it could be inferred, simplicity of the procedure, high encapsulation efficiency, high reproducibility, and low cost along with easy scaling up are considered as the advantages of the solvent-displacement technique.[11,34] Want et al. encapsulated artemisinin into PLGA nanoparticles with encapsulation efficency of 68 %. The colloidal particle showed an initial burst release, followed by a sustained release.[35] Barichello et al.[30] synthesized different drug-loaded PLGA nanoparticles using the solvent-displacement method with a particle size in the range of 160–170 nm. They studied the effect of drug type (hydrophilic, lipophilic) on encapsulation efficiency of the particles and found that the more lipophilic the drug nature was, the higher its content in the nanoparticles would be. In another work, Layre et al.[36] investigated the effect of formulation parameters on encapsulation efficiency of a crystalline drug. They concluded that the existence of high affinity between the polymer and the drug, along with choosing a dispersion medium in which drug solubility would be very low was of notable significance in obtaining increased encapsulation efficiencies of a crystalline drug. Beck-Broichsitter et al.[37] synthesized Coumarin 6-loaded PLGA nanoparticles using the solvent-displacement method. The whole dye was released after 2 h in phosphate-buffered saline (PBS) medium. Teixeira et al.[20] fabricated PLGA nanoparticles and nanospheres loaded with xanthone and 3-methoxyxanthone. The results showed that by encapsulating xanthone into nanoparticles and nanospheres, a significant initial release was observed during the first hour, followed by a slower release up to 4 h. Oyeyemi et al. fabricated PLGA polymeric nanoparticles for coencapsulation of artesunate and curcumin using solvent evaporation technique. The particle size of the nanoparticles was about 251.1 ± 12.6 nm. The in vitro drug release of the nanoparticles showed a controlled and sustained drug release over a week.[38]

For preparing particulate drug delivery systems, spray drying is considered as a relatively simple, attractive and widely used method, in which liquids (solutions, suspension, emulsions, etc.) are transformed into dried particulates.[39] This one step method is employed particularly in industrial chemistry (dispersion dyes), food industry (low-fat milk, yeast, corn starch, detergent, metal soap), cosmetics industry (olive leaf extract, beer concentrate), and pharmaceutics (blood plasma, peptides).[40] The method is used for encapsulating a wide range of materials from both water soluble and water insoluble drugs to heat resistant and heat sensitive drugs. It could be also applied for hydrophilic and hydrophobic polymers.[41–43] In general, solution or an emulsion is sprayed through a nozzle into a chamber. Simultaneously, the hot, drying air is also blown through the chamber. As the droplets meet the hot air, the residual moisture of each droplet is eliminated, leading to a transition from liquid to dried powder.[39] The physiochemical and medicinal characteristics of a powder depend on several processing variables such as feed concentration and flow rate, as well as the temperature and pressure of the drying air.[44] The resulting particle size, particle size distribution, drug encapsulation, and loading efficacy are of great importance, as it has a great impact on release, stability, physical, and pharmaceutical properties of the drug.[42,45–48] Mangrio et al.[49] produced Artemether-loaded Poly(lactic-co-glycolic) acid microparticles by coaxial electrospray method with an average size of 2 μm. The release study showed a sustained release of Artemether from core–shell structure compared to artemether.

The aim of this work is to explore the encapsulation of ART into PLGA micro- and nanoparticles in order to increase its stability and solubility as well as prevent ART from being degraded in aqueous medium. To achieve this goal, we employed two encapsulation techniques: solvent displacement and spray drying. We attempted at obtaining maximal encapsulation and loading efficacy for preventing the loss of drug and yielding a maneuverable efficient drug level. For this purpose, we employed response surface methodology (RSM) based on three-level, four parameter Box-Benkhen design (BBD). Among different design experiment methods (DOE), BBD has gained lots of interest, as it takes into account interactions of different parameters and is also time saving by reducing the number of experiments.[50] We used solvent displacement and spray drying methods; a flow chart of both methods is presented (**Figure 1**). The operating conditions were designed to tailor spherical particles with homogeneous size distribution, high drug loading, efficient encapsulation, stable particles, and optimal drug release pattern in an aqueous medium. **Figure 2** shows the chemical structure of PLGA and ART.

2. Experimental Section

2.1. Materials

PLGA 50:50 Poly (*DL*-lactide-co-glycolide) Resomer RG 503 (Molecular weight 27 000–38 000 Da) was obtained from Evonik. Artemisone was donated by CIPLA, India. Acetone, acetonitrile and Tween 80 were purchased from Sigma-Aldrich, p.a. grade and were used as received. Millipore purified water was used as an aqueous phase for preparing dispersions by solvent-displacement method.

2.2. Methods

2.2.1. Scanning Electron Microscopy and Energy Dispersive X-Ray Spectroscopy

The morphology of micro- and nanoparticles was examined by SEM using Zeiss electron microscope model LEO 1530. The
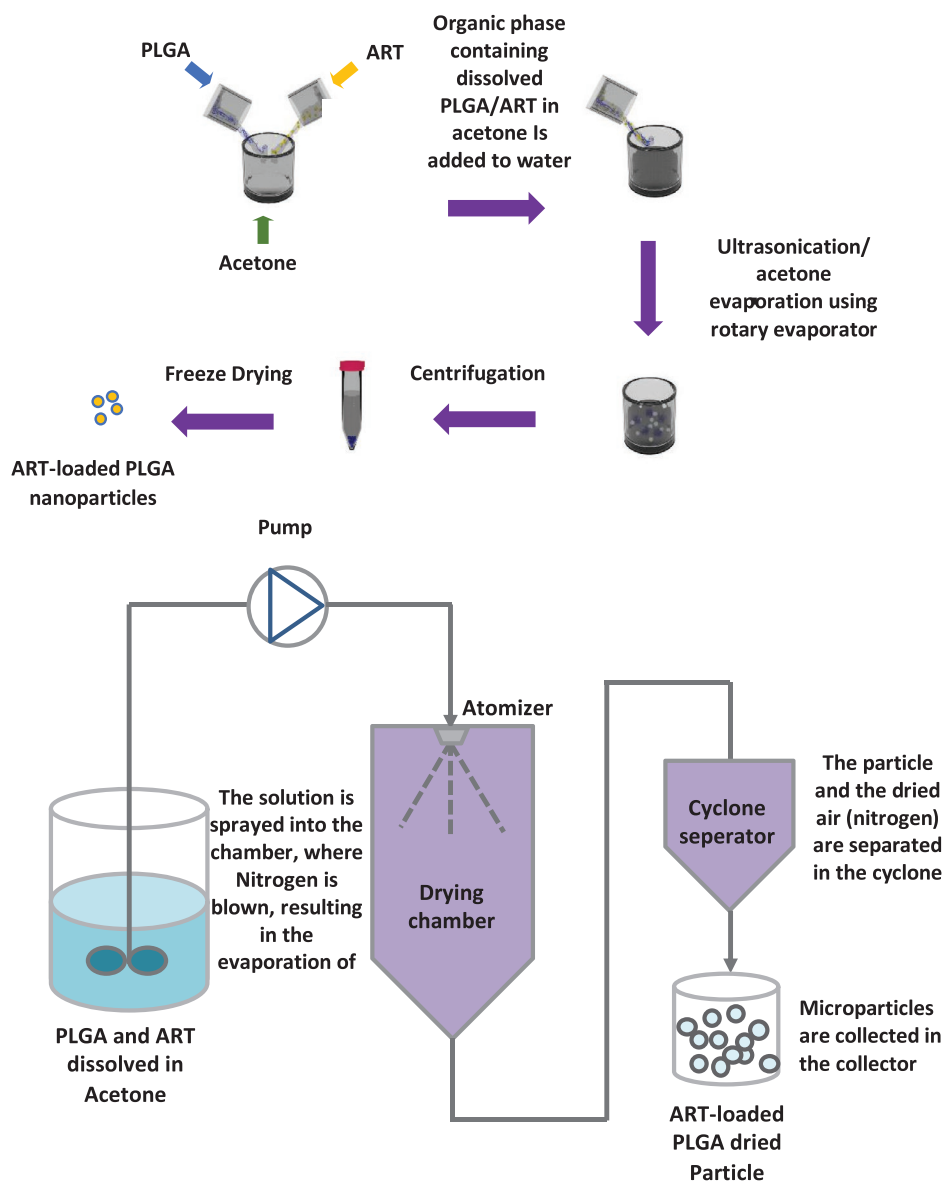
Figure 1. Solvent-displacement (up) and spray drying method (down).

average nanofiber diameter was determined by means of at least 100 random measurements using ImageJ software based on SEM images. Energy dispersive x-ray spectroscopy (EDX) analysis was done in order to characterize the presence of ART in micro- and nanoparticles.

2.2.2. X-Ray Diffraction Analysis

X-ray diffraction analysis (XRD) analysis was done in order to determine the crystallinity of the ART, PLGA and ART-loaded PLGA micro- and nanoparticles. Different samples containing the pure drug, pure polymer, and drug-loaded micro- and nanoparticles were evaluated using analytical empyrean XRD diffractometer with Cu Kα radiation (1.5418 A°).

2.2.3. Transmission Electron Microscopy

Transmission electron microscopy (TEM) was performed using Zeiss EM922 Omega EFTEM (Zeiss NTS GmbH, Oberkochen, Germany) electron microscope operated at an acceleration voltage of 200 kV. The samples were diluted with water, and then drop-coated onto a carbon-coated copper grid lying on a filter paper and were dried at room temperature overnight. The images were evaluated using Imagej.

2.2.4. Asymmetric Flow Field Flow Fractionation

Asymmetric flow field flow fractionation (AF4) was carried out in order to measure the particle size in a dispersion using NEW EAF2000 Electrical Flow FFF (Postnova). AF4 measurements
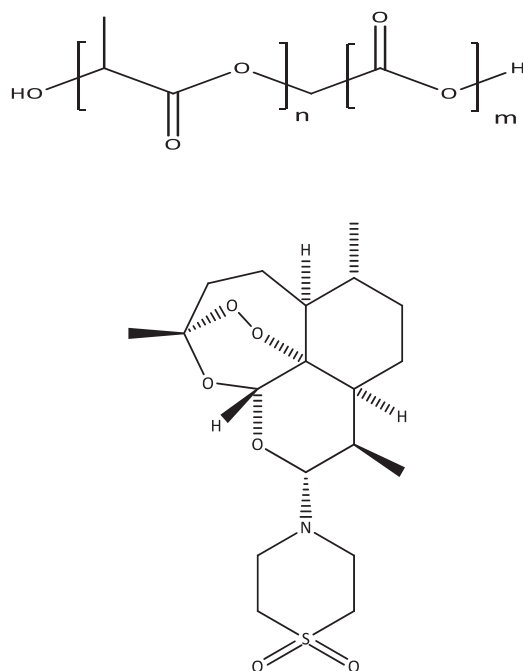
Figure 2. Chemical structure of PLGA (up) and ART (down).

were conducted using an AF2000 FFF system with a Smart Stream Splitter from Postnova with channel thickness of 350 µm and a NovaRC 10 kDa membrane. Detection was carried out by a UV detector with a maximum absorption of 525 nm and by MALS and dynamic light scattering (DLS). Water was selected as an eluent with a flow rate of 0.5 mL min^{-1}. The samples were dispersed with a concentration of 1 mg mL^{-1} in the corresponding solvent (water). In case of spray-dried microparticles, the first particles were redispersed in water using tween 80 (1% w/v) as a surfactant after which the AF4 characterization was done.

2.2.5. Dynamic Light Scattering

The mean particle size and particle size distribution were assessed by means of DLS at 25 °C using a LS spectrometer of LS Instruments AG (Fribourg, Switzerland) with HeNe laser (max. 35 mW constant output at 632.8 nm) as a source of light. The scattered light was detected using two APD detectors in pseudocross correlation. The time average scattering intensities were measured at scattering angle of 90° with an acquisition time of 60 s. Samples were diluted in water. The temperature was set with a stability of ± 100 mK by a heat controlled decalin bath. A PT100 thermoelement located close to the sample position in the decalin bath was utilized for monitoring the temperature.

2.2.6. High Performance Liquid Chromatography

High performance liquid chromatography (HPLC) was used in order to determine the amount of ART in nano- and microparticles, and to characterize the ART release from micro

and nanoparticles. This was accomplished using HPLC instrument Eclipse XDB-C18, 4.6 × 150 mm, 5 µm column Waters system equipped with autosampler AS100 and waters 2489 as UV detector. The injection volume was 20 µL. The mobile phase consisted of acetonitrile/water (60:40). The experiments were done at the wavelength of 200 nm with a flow rate of 0.8 mL min^{-1}.

2.2.7. Raman Spectroscopy

A confocal WITec alpha 300 RA+ imaging system equipped with a UHTS 300 spectrometer and a back-illuminated Andor Newton 970 EMCCD camera was employed for Raman imaging of spray-dried microparticles. Raman spectra were obtained using an excitation wavelength of λ = 532 nm, a step size of 10 pixels µm^{-1} and integration times of 0.1–0.5 s per pixel (100× objective, NA = 0.9, software WITec Control FOUR 4.1). All spectra were exposed to a cosmic ray removal routine and baseline correction.

2.2.8. Experimental Design and Data Analysis

Response surface methodology (RSM) was utilized in order to evaluate the effect of different parameters on particle size and encapsulation efficiency and optimize these parameters to get the highest encapsulation and loading efficiency. The effects of four self-determining parameters for solvent displacement method (polymer amount, drug concentration, organic to aqueous ratio, and stirrer rate) and spray drying (polymer concentration, drug concentration, flow rate and inlet temperature) on particle size and encapsulation efficiency of ART were analyzed each at three levels, coded as –1, 0, and 1, resulting in 29 experiments for each method. The version 7 of Design Expert Statistical Software was used for statistical calculations. For studying the significance of each term in the model F and P-values were investigated. P-values less than 0.05 indicate that the parameter has a significant effect.

2.2.9. Preparation of Nanoparticles Through Solvent-Displacement Method

Different amounts of polymer and drug were dissolved in organic phase consisting of acetone as a water-miscible solvent. The organic phase was then added to aqueous phase under continuous stirring thereby forming milky colloidal suspension. Afterward, the organic solvent was eliminated from the colloidal suspension using the rotary evaporator. The resultant dispersion was then centrifuged three times at 8000 rpm for 30 min in order to separate the nanoparticles from aqueous phase as well as unreacted drug.

We determined the correlation between the influence of different processing parameters on the particle size of the nanoparticles as well as drug encapsulation and loading efficiency. The parameters which were assessed were polymer amount and drug concentration, organic to aqueous ratio and stirrer rate. The aforementioned parameters along with the amounts

Table 1. Different processing parameters for solvent-displacement method.

Parameter	Amount
Polymer amount [mg]	30, 35, 40
Drug concentration [wt%]	10, 15, 20
Organic to aqueous ratio	1:2, 1:3, 1:4
Stirring rate [rpm]	250, 500, 750

are indicated in **Table 1**. The amounts of polymer and drug were selected after performing preliminary tests where no crystals of drug or no polymer layer were formed on the surface of dispersion after adding the organic phase to aqueous phase or after evaporation of the organic phase. The amount of organic to aqueous ratio and stirring rate was chosen based on the mostly used amounts in the literature.[34,51,52]

2.2.10. Preparation of Microparticles Using Spray Drying Technique

ART-loaded micro- and nanoparticles were fabricated using Spray dryer. Different concentrations of PLGA and ART were accurately weighed and dissolved in acetone. The resultant organic solutions were then spray dried using Büchi mini spray dryer B-290 (Büchi, Switzerland). Various parameters such as polymer concentration, drug concentration, flow rate, and inlet temperature were optimized to get the highest loading and encapsulation efficiencies as well as homogeneous size distribution. Aspirator level was kept constant for all trials at 100%. Operating conditions are shown in **Table 2**. The range of polymer concentration was chosen based on literature.[26,45,47] In some preliminary experiments, higher amounts resulted in inhomogeneous particle diameters and lower amounts resulted in no particle formation. Drug concentration was kept as was in the solvent-displacement method. Flow rate was chosen based on literature[53,54] and some initial experiments. Higher amounts resulted in big particles not homogeneous in size and shape. Temperature was set above acetone evaporation at levels that do not degrade ART.

2.2.11. Determination of Drug Loading and Encapsulation Efficiency

The drug encapsulation and loading efficiency were determined as explained below. For ART-loaded particles, accurately weighed dried particles were put in volumetric flask, then the solvent (acetonitrile/water, 60%v/40%v) was added and the obtained mixture was vortexed for 5 min. Afterward

Table 2. Different processing parameters for spray drying technique.

Parameter	Amount
Polymer concentration [wt%]	1, 1.5, 2
Drug concentration [wt%]	10, 15, 20
Flow rate [mL min]	1.5, 3, 4.5
Inlet temperature [°C]	61, 66, 71

the flasks were shaken for the next 45 min, the mixture was filtered using syringe filter 0.2 μm. and the dissolved ART was then injected to HPLC at a flow rate of 0.8 mL min^{-1}. Detection wavelength was set at 200 nm. The temperature of the column was kept at 35 °C. Each experiment was repeated 3 times. All results are reported as mean ± SD. Drug encapsulation and drug loading of the particles could be calculated using the following Equations (1) and (2)

$$\text{Drug encapsulation efficiency} = \frac{\text{amount of drug in nanoparticles}}{\text{initial amount of drug}} \times 100 \quad (1)$$

$$\text{Drug loading efficiency} = \frac{\text{amount of drug in nanoparticles}}{\text{weight of the nanoparticles}} \times 100 \quad (2)$$

2.2.12. Drug Release Tests

The release was measured using HPLC method that was validated by preparing ART solutions in aqueous medium containing 1 wt% tween 80.

Release tests were conducted by examining the release of ART from ART-loaded particles incubated in PBS containing 1 wt% tween 80, pH 7.4. Particle dispersion was placed in an incubator at 37 °C and at different time intervals, the dispersions were centrifuged at 10 000 rpm for 10 minutes at room temperature. Samples of the supernatants were separated and evaluated for the amount of ART released by HPLC and the same amount of solution was added in order to maintain the sink condition. The experiments were carried out in triplicate.

2.2.13. Drug Release Kinetics

To investigate the mechanism and kinetics of drug release from micro- and nanoparticles, in vitro drug release data were fitted to different kinetic models, including the zero-order model Equation (3), the first order model Equation (4), the Higuchi model Equation (5) and the Korsmeyer–Peppas model Equation (6)
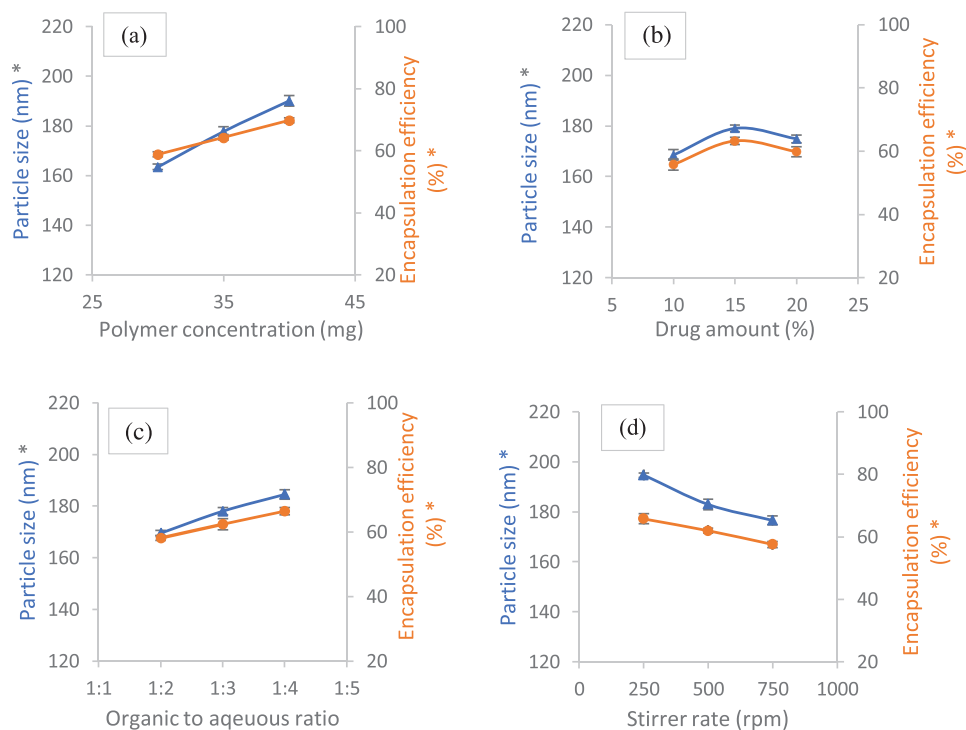
$$Q_t = K_0 t \quad (3)$$

$$\ln Q_t - \ln Q_0 = K_t t \quad (4)$$

$$Q_t = K_H \sqrt{t} \quad (5)$$

$$Q_t = K_{kp} t^n \quad (6)$$

Where t is the time, Q_t is the amount of drug released at the time t, Q_0 is the initial amount of drug in particles, K_t is the first order rate constant, K_H is Higuchi rate constant, K_{kp} is the Korsmeyer–Peppas rate constant, and n is the release exponent.[55]

ADVANCED
SCIENCE NEWS

www.advancedsciencenews.com

Particle
& Particle Systems Characterization

www.particle-journal.com

Figure 3. Effect of different parameters on particle size (→) and drug encapsulation efficiency (–●–) of ART-loaded PLGA nanoparticles prepared by solvent displacement method obtained by RSM (particle size was measured by SEM and encapsulation efficiency by HPLC). a) Polymer concentration (Drug amount 15%, Organic to aqueous ratio 1:4, Stirrer rate 500 rpm). b) Drug amount (Polymer concentration 35 mg, Organic to aqueous ratio 1:4, Stirrer rate 500 rpm). c) Organic to aqueous ratio (Polymer concentration 35 mg, Drug amount 15%, Stirrer rate 500 rpm). d) Stirrer rate (Polymer concentration 35 mg, Drug amount 15%, Organic to aqueous ratio 1:4). *P-values for particle size: Polymer concentration (0.0001), drug concentration (0.4091), organic to aqueous ratio (0.005), stirrer rate (0.0012). *P-values for encapsulation efficiency: Polymer concentration (<0.0001), drug concentration (<0.0001), organic to aqueous ratio (<0.0001), stirrer rate (<0.0001).
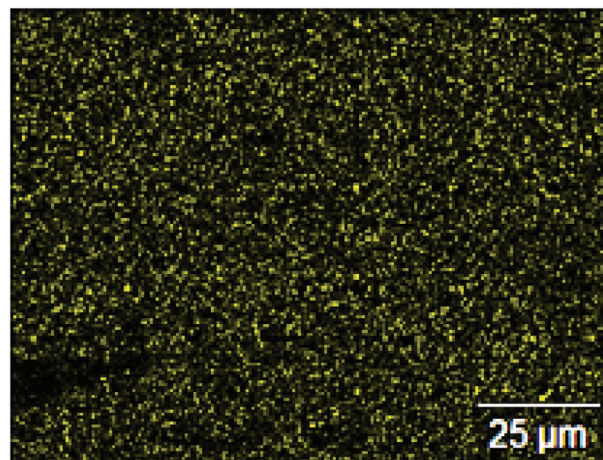
2.2.14. Statistical Analysis

All data were reported as mean ± standard deviation (SD). Statistical analysis was done by one-way analysis of variance (ANOVA).

3. Results and Discussion

Different parameters may affect particle size and encapsulation efficiency while using solvent displacement and spray drying methods. In order to be able to interpret and compare
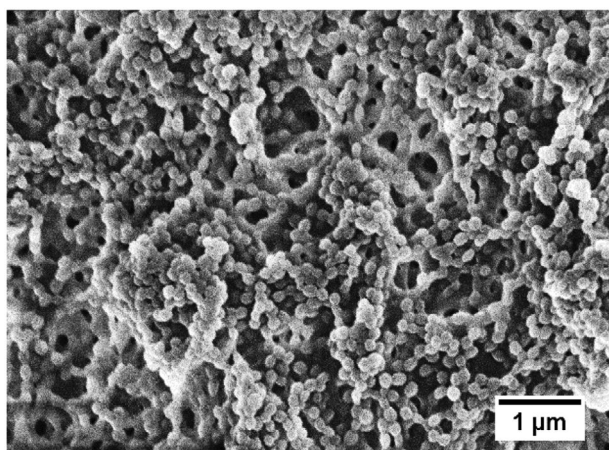
Figure 4. SEM micrographs of ART-loaded nanoparticles by solvent-displacement method.

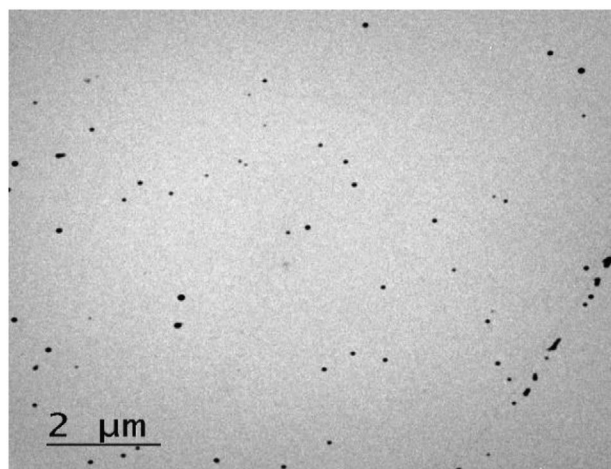**Figure 5.** Representative EDX image of ART-loaded PLGA nanoparticles.

**ADVANCED
SCIENCE NEWS**
www.advancedsciencenews.com

Particle
& Particle Systems Characterization
www.particle-journal.com

Figure 6. TEM image of ART-loaded PLGA nanoparticle dispersion.

our results in a more efficient way, we summarized the results of the effect of parameters on particle size and encapsulation efficiency for solvent displacement method and spray drying in Tables S1 and S2 (Supporting Information).

3.1. ART Encapsulated into PLGA Matrix Produced by the Solvent Displacement Method

We used PLGA 50:50, which is characterized by a comonomer ratio of 50% *DL*-lactide and 50% glycolide and a molecular weight of 38 000 g mol^{-1}. Different parameters that may influence particle size and morphology as well as the encapsulation efficiency were investigated: polymer concentration in the solution, drug concentration, organic to aqueous ratio and stirrer rate. **Figure 3** presents the effect of these parameters on particle size and encapsulation efficiency of ART-loaded nanoparticles fabricated by solvent displacement. Polymer concentration is regarded as a critical factor governing the particle size that is vital for drug delivery applications.[56,57] Similarly, it was observed in this work that polymer concentration plays an important role in determining drug encapsulation efficiency and size of nanoparticle (Figure 3a). Increasing the polymer concentration resulted in significant increase in particle size (from 160 to 190 nm). This is in agreement with the literature.[58] In general, the higher polymer–polymer interaction hinder the diffusion of solvent into aqueous phase, thereby yielding nanoparticles larger in size.[18] In addition, as the polymer concentration is enhanced, the encapsulation and loading efficiency increases (from 58% to 70%). This could be ascribed to the fact that the greater the polymer concentration is, the higher the particle size would be. Considering this, an increment in the diameter of the particles brings about a decrease in surface to volume ratio, therefore lowering the chance of drug leakage through diffusional routes to the aqueous medium and resulting in higher encapsulation efficiencies.[59]

Increasing the drug concentration yielded a slight increase in nanoparticle size (from 170 to 178 nm) as well as encapsulation (from 55% to 61%) followed by a decrease to 174 nm and 59%, respectively (Figure 3b). It is in accordance with the conclusion

of Budhian et al.:[56] "Increasing the drug amount increases the resistance to diffusion of solvent into aqueous phase, which results in higher particle size."

Figure 3c presents the effect of organic to aqueous ratio on particle size and encapsulation efficiency. A rise in encapsulation efficiency (from 58% to 66%) as well as particle size (from 170 to 184 nm) was found with decreasing organic to aqueous ratio: increasing the amount of organic to water ratio facilitates the diffusion of the solvent into the aqueous phase, consequently decreasing the particles size and increasing the surface area as well as leading to better partitioning of the drug in the aqueous phase, and ultimately causing a decrease in encapsulation efficiency.[18,60]

Increasing the stirring rate (Figure 3d) resulted in a decrease in particle size (from 195 to 175 nm). The data are in agreement with the literature.[58,61] As described in the previous paragraph, the particle formation is mainly based on the diffusion of organic phase into aqueous phase, consequently, particle formation owing to solvent diffusion is time-dependent. Once the stirring rate is low, the probability that the organic phase would rapidly diffuse into the aqueous phase is lower.[61,62] By increasing the stirrer rate, which results in reducing the time it takes for the drug to diffuse, diffusion hindrance might take place, resulting in a slight decreased amount of drug, which is encapsulated in nanoparticles (from 65% to 57%).[56]
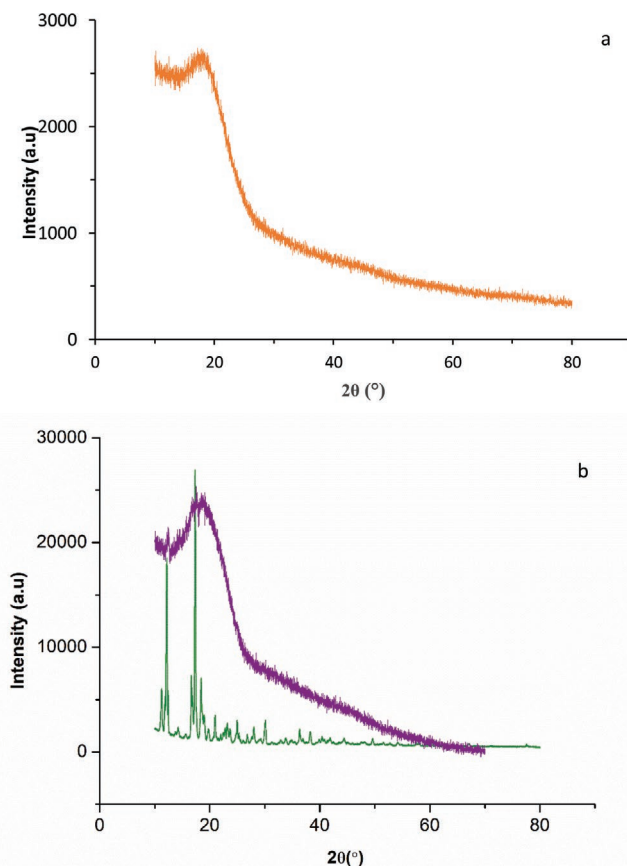

Figure 7. XRD pattern of a) PLGA (———), b) ART and ART-loaded PLGA nanoparticles produced by solvent displacement. (———) shows ART and (———) ART-loaded PLGA nanoparticles.

The data regarding SEM and HPLC for particle size and encapsulation efficiency was given in RSM and used to evaluate and optimize the effect of different parameters. Based on the RSM results for particle size, polymer amount, organic to aqueous ratio and stirrer rate are the most influential parameters ($P < 0.05$). For encapsulation efficiency, all four parameters including polymer amount, drug concentration, organic to aqueous ratio and stirrer rate are significant ($P < 0.05$). Additionally, as it could be deduced from Figure 3, polymer concentration plays the most important role in affecting particle size and encapsulation efficiency.

The optimized conditions, in which the highest encapsulation efficiency is achieved, were chosen based on RSM to prepare nanoparticles for further use. The optimized conditions are as following: Polymer amount 40 mg, drug concentration 20 wt%, organic to aqueous ratio 1:4 and stirrer rate 250 rpm. When using the optimized condition, the highest encapsulation efficiency was 71% with a loading efficiency of ≈14.2% with an average particle diameter of 173 ± 15 nm as determined by DLS. The AFFF results represents a particle diameter of 171 ± 10 nm, which is in complement agreement with both the DLS and SEM results. SEM micrographs demonstrated round particles homogenous in size (average particle size: 160 ± 18 nm). A slightly higher particle size for DLS and AFFF could be found due to the fact that for these two analyses the particles are present in an aqueous medium, resulting in a difference as compared to SEM micrograph, in which particles are measured in a dried state (**Figure 4**).

The distribution of ART in the nanoparticles was evaluated using energy dispersive X-ray analysis (EDX) by tracking its characteristic element, sulfur, in nanoparticles (**Figure 5**).

TEM micrographs of ART-loaded nanoparticles (**Figure 6**) confirm the spherical shape of nanoparticles along with homogeneous size distribution. Moreover, it is also observable that the particles are not agglomerated to each other, showing their good dispersion and stability in water without using any surfactant. The average particle size achieved by TEM is in great agreement with that of SEM, DLS, and AFFF measurements.

XRD patterns (**Figure 7**) show that ART-loaded nanoparticles exhibit two characteristic low intensity peaks at 11.25° and 17.34°, which could be attributed to the characteristic crystalline peaks of the ART.[63] It could be concluded that the drug has slightly retained its crystalline structure, but still demonstrating high encapsulation efficiencies which was proved by using HPLC.
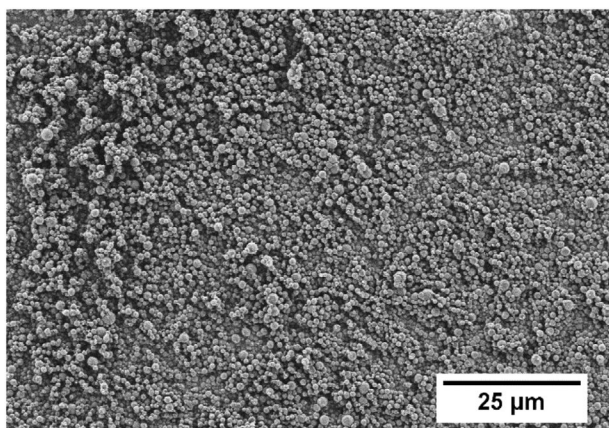
3.2. ART Encapsulated into PLGA Matrix Produced by the Spray Drying Method

The effect of different parameters on particle size and encapsulation efficiency of the ART-loaded particles prepared by spray drying method were obtained by RSM methodology (**Figure 8**). Higher polymer concentrations contributed to significant increase in particle size (from 1 to 1.7 µm) (Figure 8a).[47]
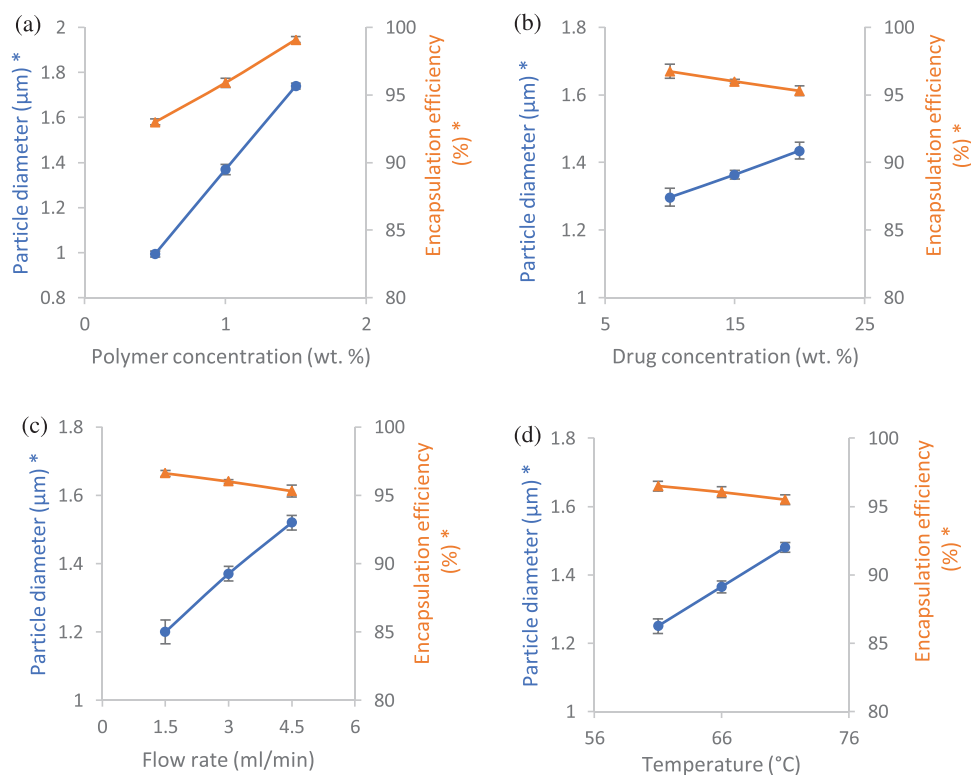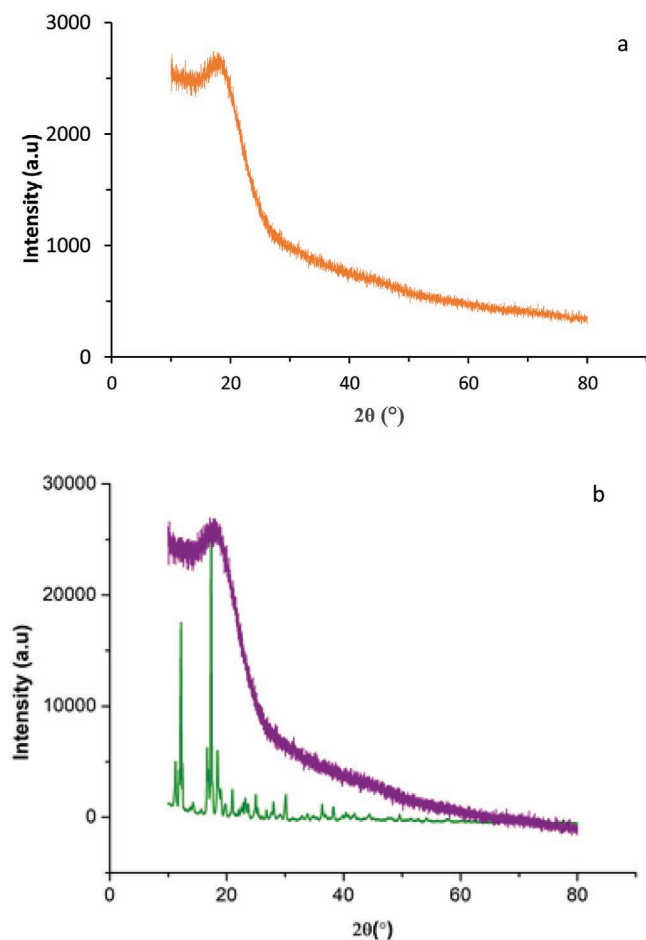

Figure 8. Effect of different parameters on particle size (—▲—) and drug encapsulation efficiency (—●—) of ART-loaded PLGA microparticles prepared by spray drying method obtained by RSM (particle size was measured by SEM and encapsulation efficiency by HPLC), namely. a) Polymer concentration (Drug concentration 15%, Flow rate 3 mL min⁻¹, Temperature 66°). b) Drug concentration (Polymer concentration 1%, Flow rate 3 mL min⁻¹, Temperature 66°). c) Flow rate (Polymer concentration 1%, drug concentration 15%, Temperature 66°). d) Temperature (Polymer concentration 1%, drug concentration 15%, Flow rate 3 mL min⁻¹).

**ADVANCED
SCIENCE NEWS**
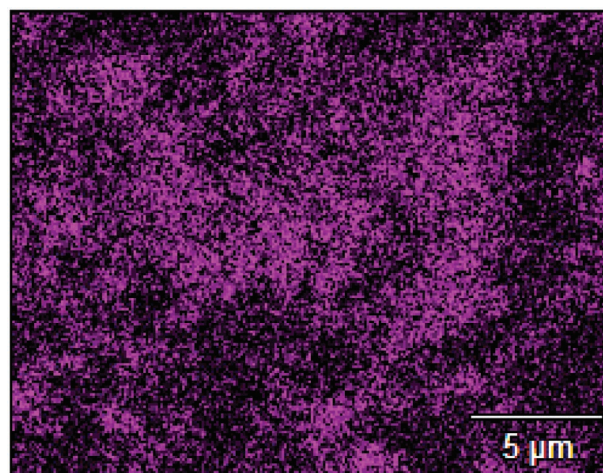
www.advancedsciencenews.com

Particle
& Particle Systems Characterization

www.particle-journal.com

Figure 9. SEM analysis of ART loaded PLGA microparticles prepared by spray-dried method.

Figure 11. Representative EDX spectrum of spray-dried ART-loaded PLGA microparticles.

Consequently, a higher degree of drug encapsulation (from 92% to 99%) was observed for the higher polymer content. Obviously, a rise in the solid amount of each droplet, results in increased particle size and encapsulation efficiency. In addition, as the polymer amount increases, the


Figure 10. XRD pattern of a) PLGA (——), b) ART (——), and (——) ART-loaded PLGA microparticles produced by spray drying shows ART and ART-loaded PLGA microparticles.

possibility that the drug would be exposed to the particle surface decreases and in turn the encapsulation efficiency is elevated.[40] Also, a change in the crystalline nature of drug into amorphous state following increase in polymer content, could also happen.[39]

Keeping the polymer concentration constant, higher drug concentrations resulted in a minimal increase in particle size (from 1.3 to 1.45 µm) (Figure 8b). Following an increase of flow rate there was an increase in droplet size due to the fact that larger droplets were formed during spray drying process, because more liquid is sprayed thorough the nozzle.[64] Consequently, particle size was also increased (from 1.2 to 1.5 µm, Figure 8c). However, as there would not be enough time for the drug to be encapsulated into particles as a result of higher flow rate, this would result in a slight decrease of encapsulation efficiency (from 96.5% to 95%). An increase in the inlet temperature (Figure 8d) resulted in a slight increase (from 1.25 to 1.45 µm) in particle size. Increasing the inlet temperature could result in a faster formation of particle structure, consequently hindering the shrinkage of particles during drying process and
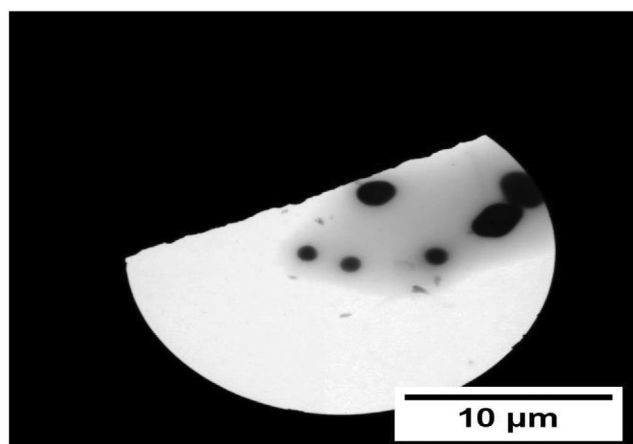
Figure 12. TEM micrographs of ART-loaded PLGA spray dried microparticles in water containing 1 wt% Tween 80.
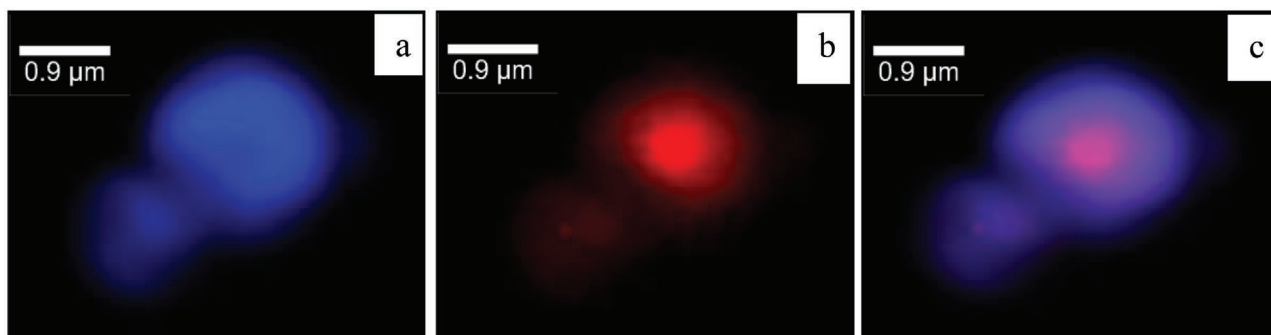
Figure 13. Raman image of a) PLGA distribution, b) ART distribution, c), combined distribution of PLGA and ART.

resulting in higher diameter of particles, accordingly.[46,65] On the other hand, a decrease in the encapsulation efficiency (from 96.5% to 95.5%) could be related to the fact that higher temperatures give rise to a faster drying of the solvent, as a result there wouldn't be enough time for the drug to be encapsulated, allowing only partial encapsulation.[66]

Based on the RSM results, for particle size polymer concentration, flow rate and inlet temperature and for encapsulation efficiency, all four parameters including polymer concentration, drug concentration, flow rate and inlet temperature are significant ($P < 0.05$). It could be also concluded from the ANOVA results that among the different parameters, polymer concentration has the most effect on both particle size and encapsulation efficiency of the particles. For spray drying method, only for changes in polymer concentration, the same trend was observed in particle size and encapsulation efficiency. For other parameters, an increase in their amount resulted in converse effects in both particle size and encapsulation efficiency.

The optimal conditions, in which the highest encapsulation efficiency is achieved are as following: Polymer concentration 15 wt%, drug concentration 15 wt%, flow rate 4.5 mL h^{-1}, and temperature 61 °C and were chosen to prepare microparticles for further use.

Microparticles with high encapsulation efficiencies of 97% and average particle diameter of 1400 ± 550 nm (**Figure 9**). For AFFF analysis, microparticles were redispersed in Tween 80. The average size obtained by AFFF was 1270 ± 30.

ART alone was found to be completely crystalline (**Figure 10**), exhibiting diffraction peaks at 11.25°, 12.18°, 16.66°, 17.34°, 18.43°, and 25.34°, respectively.[63] According to Figure 9, no crystalline peak was detected in ART-loaded PLGA microparticles. This could be ascribed to the fact that the encapsulation of the drug in the PLGA which is an amorphous polymer also resulted in particles with an amorphous structure. This correlates with a situation where the drug is entirely encapsulated inside polymeric microparticles,[47] proving high encapsulation efficiencies of more than 97%, which is also in agreement with Raman findings.

EDX was carried out in order to locate ART in ART-loaded microparticles (**Figure 11**). The EDX micrograph illustrates the presence of elemental sulfur, which exists in the structure of ART and indicates the homogenous distribution of ART in the microparticles.

Tween 80 was used in order to redisperse particles in water. The drug-loaded microparticles are evenly redispersed in water

and Tween 80 as a stabilizing surfactant, and mostly kept their round structure (**Figure 12**). The average particle size gained was in a range of 1700 ± 500 nm, which is slightly higher than that found by SEM. This could be due to the presence of Tween 80 that binds to the particle surface. Other surfactants, SDS and PVA were used, but it did not result in a stable dispersion and the particles were precipitated.

Raman spectroscopy was conducted to investigate whether the drug is completely encapsulated into the microparticles or just located on their surface (**Figure 13**). The distribution of PLGA and ART as well as the combined distribution of both components. It is clear that the drug is completely encapsulated inside the polymer matrix. These results go hand in hand with the XRD results, which already proved that ART is entirely encapsulated into the polymer matrix.

Release pattern of drug from drug-loaded micro and nanoparticles is highly important due to its potential effect on the applicability of the product.[67] The time dependence of drug release was analyzed from micro- and nanoparticles containing 14 wt % ART (**Figure 14**). For nanoparticles a burst release of about 60% was observed within 30 min and the whole drug was released after two and half hours. In contrast, for ART-loaded microparticles within 30 min only 20% of the drug was released, followed by a slower release during up to 22 h.
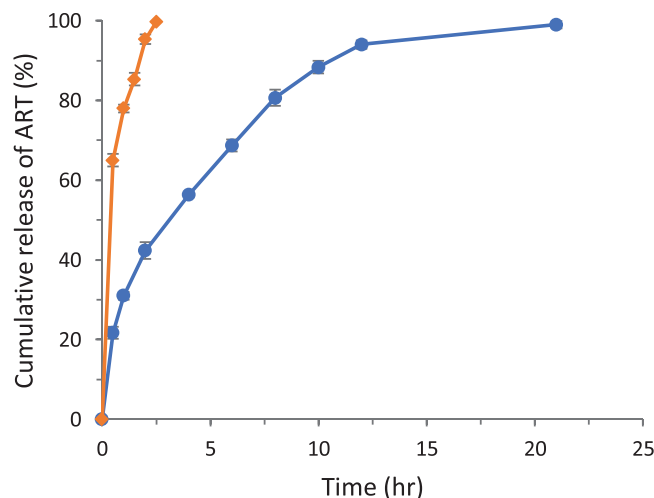
Figure 14. ART release from ART-loaded PLGA micro (━●━) and nanoparticle (━◆━) synthesized using spray drying and solvent-displacement method, respectively.

Table 3. Release parameters for ART-loaded PLGA micro- and nanoparticles obtained by fitting in vitro drug release data to various models for drug release kinetics.

Particle type	Zero order		First order		Higuchi		Korsmeyer–Peppas		
	R^2	K	R^2	K	R^2	K	R^2	K	n
Nanoparticle	0.9798	7.54×10^{-1}	0.9785	1.5×10^{-2}	0.9876	3.845	0.9978	3.7×10^{-1}	0.59
Microparticle	0.9705	2.8×10^{-2}	0.9627	1.4×10^{-3}	0.9805	0.589	0.9948	9.8×10^{-2}	0.49

These results could be attributed to the longer diffusion path of the drug within microparticles compared to the nanoparticles. However, based on XRD, the drug is not completely encapsulated in nanoparticles, meaning that there are some fractions of drug available on the surface of nanoparticle, whereas in the case of spray-dried microparticles it was proved not only through XRD, but also by using novel Raman technique that the whole drug is encapsulated within microparticles and not located on the surface, consequently resulting in a preferable release.

To investigate the drug release kinetics, the data were fitted into four different models such as Zero-order, First-order, Higuchi and Korsmeyer–Peppas model for both micro- and nanoparticles. Based on our results, the Korsmeyer–Peppas model has the highest correlation Coefficient for both microparticles $R^2 = 0.9948$ and for nanoparticles $R^2 = 0.9978$ (**Table 3**). For this analysis, the data in the range of 5–60% of drug released were used. Additionally, the amount of *n* which is obtained for both microparticles 0.49 and nanoparticles 0.59 is between 0.5 and 1 showing that the release mechanism is anomalous transport or non-Fickian diffusion, which means the release is a combination of diffusion and dissolution.[35,55]

4. Conclusion

In this work, ART-loaded nano- and microparticles were successfully and reproducibly synthesized using solvent-displacement and spray drying technique, respectively. The major step forward using these two methods is a successful production of spherical micro- and nanoparticles with high encapsulation and loading efficiencies. We optimized systematically both methods by examining different parameters that may influence particle size and encapsulation efficiency of the particles. For both methods, it was concluded that polymer concentration has the most influence on particle size and encapsulation efficiency. A more sustained release of ART was observed for microparticles due to complete encapsulation of drug, which was ascertained by Raman, in comparison to the noticeable immediate burst release for the nanoparticles.

Altogether, we developed easy to produce stable nanoparticle dispersions and dried microparticle powder, with a spherical shape, high encapsulation efficiencies, high drug loadings and methods that enable burst or slow release, as needed. The formulations might be applied in diseases where treatment by artemisinins is efficient, for example cancer,[68–70] malaria, and schistosomiasis.[9,71] Formulations of other lipophilic drugs using solvent displacement, and water-soluble as well as water-insoluble drugs using spray drying method might be produced using identical methods.

Supporting Information

Supporting Information is available from the Wiley Online Library or from the author.

Conflict of Interest

The authors declare no conflict of interest.

Data Availability Statement

The data that support the findings of this study are available in the supplementary material of this article.

[1] E. A. Ashley, A. Pyae Phyo, C. J. Woodrow, *Lancet* **2018**, *391*, 1608.

[2] C. A. Moxon, M. P. Gibbins, D. McGuinness, D. A. Milner, M. Marti, *Annu. Rev. Pathol. Mech. Dis.* **2020**, *15*, 315.

[3] World Malaria Report 2020: 20 years of Global Progress and Challenges. Geneva: World Health Organization; 2020. Licence: CC BY-NC-SA 3.0 IGO.

[4] J. Golenser, V. Buchholz, A. Bagheri, A. Nasereddin, R. Dzikowski, J. Guo, N. H. Hunt, S. Eyal, N. Vakruk, A. Greiner, *Parasit. Vectors* **2017**, *10*, 117.

[5] J. Nagelschmitz, B. Voith, G. Wensing, A. Roemer, B. Fugmann, R. K. Haynes, B. M. Kotecka, K. H. Rieckmann, M. D. Edstein, *Antimicrob. Agents Chemother.* **2008**, *52*, 3085.

[6] R. K. Haynes, B. Fugmann, J. Stetter, K. Rieckmann, H.-D. Heilmann, H.-W. Chan, M.-K. Cheung, W.-L. Lam, H.-N. Wong, S. L. Croft, L. Vivas, L. Rattray, L. Stewart, W. Peters,

B. L. Robinson, M. D. Edstein, B. Kotecka, D. E. Kyle, B. Beckermann, M. Gerisch, M. Radtke, G. Schmuck, W. Steinke, U. Wollborn, K. Schmeer, A. Römer, *Angew. Chem., Int. Ed.* **2006**, *45*, 2082.

[7] A. R. Bagheri, S. Agarwal, J. Golenser, A. Greiner, *Global Challenges* **2017**, *1*, 1600011.

[8] A. R. Bagheri, J. Golenser, A. Greiner, *Eur. Polym. J.* **2020**, *129*, 109625.

[9] J. Zech, N. Salaymeh, N. H. Hunt, K. Mäder, J. Golenser, *Antimicrob. Agents Chemother.* **2021**, *65*, e02106.

[10] A. Guasch-Girbau, X. Fernàndez-Busquets, *Pharmaceutics* **2021**, *13*, 2189.

[11] K. Avgoustakis, *Curr. Drug Delivery* **2004**, *1*, 321.

[12] E. Sayed, R. Haj-Ahmad, K. Ruparelia, M. S. Arshad, M.-W. Chang, Z. Ahmad, *AAPS PharmSciTech* **2017**, *18*, 1507.

[13] M. Sheikhpour, L. Barani, A. Kasaeian, *J. Controlled Release* **2017**, *253*, 97.

[14] N. Teekamp, L. F. Duque, H. W. Frijlink, W. L. Hinrichs, P. Olinga, *Expert Opin. Drug Delivery* **2015**, *12*, 1311.

[15] K. S. Soppimath, T. M. Aminabhavi, A. R. Kulkarni, W. E. Rudzinski, *J. Controlled Release* **2001**, *70*, 1.

[16] S. Patra, M. Singh, K. Wasnik, D. Pareek, P. S. Gupta, S. Mukherjee, P. Paik, *ACS Appl. Bio Mater.* **2021**, *4*, 7342.

[17] E. Andronescu, A. M. Grumezescu, *Nanostructures for Drug Delivery*, Elsevier, amsterdam **2017**.

[18] S. A. Guhagarkar, V. C. Malshe, P. V. Devarajan, *AAPS PharmSciTech* **2009**, *10*, 935.

[19] A. O. Elzoghby, W. M. Samy, N. A. Elgindy, *J. Controlled Release* **2012**, *157*, 168.

[20] M. Teixeira, M. J. Alonso, M. M. M. Pinto, C. M. Barbosa, *Eur. J. Pharm. Biopharm.* **2005**, *59*, 491.

[21] D. S. Kohane, *Biotechnol. Bioeng.* **2007**, *96*, 203.

[22] A. Hussain, S. Singh, S. S. Das, K. Anjireddy, S. Karpagam, F. Shakeel, *Curr. Drug Delivery* **2019**, *16*, 400.

[23] F. Molavi, M. Barzegar-Jalali, H. Hamishehkar, *J. Controlled Release* **2020**, *320*, 265.

[24] M. L. Hans, A. M. Lowman, *Curr. Opin. Solid State Mater. Sci.* **2002**, *6*, 319.

[25] K. Anwer, M. Mohammad, E. Ezzeldin, F. Fatima, A. Alalaiwe, M. Iqbal, *Int. J. Nanomed.* **2019**, *14*, 1587.

[26] M. D. Blanco, R. L. Sastre, C. Teijón, R. Olmo, J. M. Teijón, *J. Microencapsul.* **2005**, *22*, 671.

[27] K. Dauda, Z. Busari, O. Morenikeji, F. Afolayan, O. Oyeyemi, J. Meena, D. Sahu, A. Panda, *J. Zhejiang Univ.- Sci. B* **2017**, *18*, 977.

[28] S. Freiberg, X. X. Zhu, *Int. J. Pharm.* **2004**, *282*, 1.

[29] A. George, P. A. Shah, P. S. Shrivastav, *Int. J. Pharm.* **2019**, *561*, 244.

[30] J. M. Barichello, M. Morishita, K. Takayama, T. Nagai, *Drug Dev. Ind. Pharm.* **1999**, *25*, 471.

[31] E. Piñón-Segundo, A. Ganem-Quintanar, J. Rafael Garibay-Bermúdez, J. Juan Escobar-Chávez, M. López-Cervantes, D. Quintanar-Guerrero, *Pharm. Dev. Technol.* **2006**, *11*, 493.

[32] C. Pinto Reis, R. J. Neufeld, A. J. Ribeiro, F. Veiga, *Nanomed. Nanotechnol. Biol. Med.* **2006**, *2*, 8.

[33] H. Murakami, M. Kobayashi, H. Takeuchi, Y. Kawashima, *Int. J. Pharm.* **1999**, *187*, 143.

[34] C. E. Mora-Huertas, H. Fessi, A. Elaissari, *Adv. Colloid Interface Sci.* **2011**, *163*, 90.

[35] M. Y. Want, M. Islamuddin, G. Chouhan, A. K. Dasgupta, A. P. Chattopadhyay, F. Afrin, *J. Colloid Interface Sci.* **2014**, *432*, 258.

[36] A.-M. Layre, R. Gref, J. Richard, D. Requier, H. Chacun, M. Appel, A. J. Domb, P. Couvreur, *Int. J. Pharm.* **2005**, *298*, 323.

[37] M. Beck-Broichsitter, M. Thieme, J. Nguyen, T. Schmehl, T. Gessler, W. Seeger, S. Agarwal, A. Greiner, T. Kissel, *Macromol. Biosci.* **2010**, *10*, 1527.

[38] O. Oyeyemi, O. Morenkeji, F. Afolayan, K. Dauda, Z. Busari, J. Meena, A. Panda, *Front. Pharmacol.* **2018**, *9*, 562.

[39] M.-I. Ré, *Dry Technol.* **2006**, *24*, 433.

[40] X. Li, N. Anton, C. Arpagaus, F. Belleteix, T. F. Vandamme, *J. Controlled Release* **2010**, *147*, 304.

[41] A. H. Salama, *Drug Delivery Transl. Res.* **2020**, *10*, 1.

[42] L. Mu, S. S. Feng, *J. Controlled Release* **2001**, *76*, 239.

[43] P. Giunchedi, B. Conti, I. Genta, U. Conte, G. Puglisi, *Drug Dev. Ind. Pharm.* **2001**, *27*, 745.

[44] H. Yamamoto, W. Hoshina, H. Kurashima, H. Takeuchi, Y. Kawashima, T. Yokoyama, H. Tsujimoto, *Adv. Powder Technol.* **2007**, *18*, 215.

[45] C. Draheim, F. de Crécy, S. Hansen, E.-M. Collnot, C.-M. Lehr, *Pharm. Res.* **2015**, *32*, 2609.

[46] R. V. Tonon, C. R. F. Grosso, M. D. Hubinger, *Food Res. Int.* **2011**, *44*, 282.

[47] N. Schafroth, C. Arpagaus, U. Y. Jadhav, S. Makne, D. Douroumis, *Colloids Surf., B* **2012**, *90*, 8.

[48] R. V. Tonon, S. S. Freitas, M. D. Hubinger, *J. Food Process. Preserv.* **2011**, *35*, 691.

[49] F. A. Mangrio, P. Dwivedi, S. Han, G. Zhao, D. Gao, T. Si, R. X. Xu, *Mol. Pharmaceutics* **2017**, *14*, 4725.

[50] M. Heidari, H. Bahrami, M. Ranjbar-Mohammadi, *Mater. Sci. Eng. C* **2017**, *78*, 218.

[51] J. Cheng, B. Teply, I. Sherifi, J. Sung, G. Luther, F. Gu, E. Levynissenbaum, A. Radovicmoreno, R. Langer, O. Farokhzad, *Biomaterials* **2007**, *28*, 869.

[52] C. Duclairoir, E. Nakache, H. Marchais, A.-M. Orecchioni, *Colloid Polym. Sci.* **1998**, *276*, 321.

[53] Y.-J. Fu, S.-S. Shyu, F.-H. Su, P.-C. Yu, *Colloids Surf., B* **2002**, *25*, 269.

[54] H. Adi, P. M. Young, H.-K. Chan, P. Stewart, H. Agus, D. Traini, *J. Pharm. Sci.* **2008**, *97*, 3356.

[55] V. Chourasiya, S. Bohrey, A. Pandey, *Mater. Discovery* **2016**, *5*, 1.

[56] A. Budhian, S. J. Siegel, K. I. Winey, *Int. J. Pharm.* **2007**, *336*, 367.

[57] W. Badri, K. Miladi, Q. A. Nazari, H. Fessi, A. Elaissari, *Colloids Surf., A* **2017**, *516*, 238.

[58] K. Y. Hernández-Giottonini, R. J. Rodríguez-Córdova, C. A. Gutiérrez-Valenzuela, O. Peñuñuri-Miranda, P. Zavala-Rivera, P. Guerrero-Germán, A. Lucero-Acuña, *RSC Adv.* **2020**, *10*, 4218.

[59] E. Vega, M. A. Egea, O. Valls, M. Espina, M. L. García, *J. Pharm. Sci.* **2006**, *95*, 2393.

[60] C. Fonseca, S. Simões, R. Gaspar, *J. Controlled Release* **2002**, *83*, 273.

[61] T. B. Tan, N. S. Yussof, F. Abas, H. Mirhosseini, I. A. Nehdi, C. P. Tan, *Food Chem.* **2016**, *194*, 416.

[62] H. Asadi, K. Rostamizadeh, D. Salari, M. Hamidi, *J. Microencapsul.* **2011**, *28*, 406.

[63] H. Yu, X. Zhao, Y. Zu, X. Zhang, B. Zu, X. Zhang, *Int. J. Mol. Sci.* **2012**, *13*, 5060.

[64] A. L. R. Rattes, W. P. Oliveira, *Powder Technol.* **2007**, *171*, 7.

[65] J. Toro-Sierra, J. Schumann, U. Kulozik, *Dairy Sci. Technol.* **2013**, *93*, 487.

[66] M. N. Lavanya, T. Kathiravan, J. A. Moses, C. Anandharamakrishnan, *Dry. Technol.* **2020**, *38*, 279.

[67] N. Kamaly, B. Yameen, J. Wu, O. C. Farokhzad, *Chem. Rev.* **2016**, *116*, 2602.

[68] B. Aderibigbe, *Molecules* **2017**, *22*, 323.

[69] Z. Guo, *Acta Pharm. Sin. B* **2016**, *6*, 115.

[70] S. Alven, B. A. Aderibigbe, *Pharmaceutics* **2020**, *12*, 748.

[71] J. Zech, D. Gold, N. Salaymeh, N. C. Sasson, I. Rabinowitch, J. Golenser, K. Mäder, *Pharmaceutics* **2020**, *12*, 509.